DOI: 10.1161/CIRCGENETICS.115.001323

Spectrum and Prevalence of *CALM1*-, *CALM2*-, and *CALM3*-Encoded Calmodulin (CaM) Variants in Long QT Syndrome (LQTS) and Functional Characterization of a Novel LQTS-Associated CaM Missense Variant, E141G

Running title: *Boczek et al.; Calmodulin and LQTS*

Nicole J. Boczek, PhD[1]*; Nieves Gomez-Hurtado, PhD[2]*; Dan Ye, MD[1]*; Melissa L. Calvert, BS[1]; David J. Tester, BS[1]; Dmytro Kryshtal, PhD[2]; Hyun Seok Hwang, PhD[2]; Christopher N. Johnson, PhD[3]; Walter J. Chazin, PhD[3]; Christina G. Loporcaro, BS[1,4]; Maully Shah, MD[5]; Andrew L. Papez, MD[6]; Yung R. Lau, MD[7]; Ronald Kanter, MD[8]; Bjorn C. Knollmann, MD, PhD[2]; Michael J. Ackerman, MD, PhD[1,9-10]

[1]Department Molecular Pharmacology & Experimental Therapeutics, Windland Smith Rice Sudden Death Genomics Laboratory, [4]Mayo Medical School, [9]Department of Medicine, Division of Cardiovascular Diseases, [10]Department of Pediatrics, Division of Pediatric Cardiology, Mayo Clinic, Rochester, MN; [2]Department of Medicine, [3]Departments of Biochemistry & Chemistry and Center for Structural Biology, Vanderbilt University, Nashville, TN; [5]Children's Hospital of Philadelphia, Philadelphia, PA; [6]Department of Pediatric Cardiology, Phoenix Children's Hospital, Phoenix, AZ; [7]Department of Pediatrics, Division of Pediatric Cardiology, University of Alabama at Birmingham, Birmingham, AL; [8]Division of Cardiology, Nicklaus Children's Hospital, Miami, FL
*contributed equally as first authors

Correspondence:

Michael J. Ackerman, MD, PhD
Mayo Clinic Windland Smith Rice
Sudden Death Genomics Laboratory
Guggenheim 501, Mayo Clinic
200 First Street SW,
Rochester, MN 55905
Tel: 507-284-0101
Fax: 507-284-3757
E-mail: ackerman.michael@mayo.edu

Björn C. Knollmann, MD, PhD
Professor of Medicine and Pharmacology,
Division of Clinical Pharmacology
Vanderbilt University School of Medicine
Medical Research Building IV, Rm. 1265
2215B Garland Ave., Nashville, TN 37232-0575
Tel: (615) 343-6493
Fax: (615) 343-4522
E-mail: bjorn.knollmann@vanderbilt.edu

Journal Subject Terms: Arrhythmias; Ion Channels/Membrane Transport; Genetics

DOI: 10.1161/CIRCGENETICS.115.001323

Abstract:

Background - Calmodulin (CaM) is encoded by three genes, *CALM1, CALM2,* and *CALM3,* all of which harbor pathogenic variants linked to long QT syndrome (LQTS) with early and severe expressivity. These LQTS-causative variants reduce CaM affinity to Ca^{2+} and alter the properties of the cardiac L-type calcium channel ($Ca_V1.2$). CaM also modulates $Na_V1.5$ and the ryanodine receptor, RyR2. All of these interactions may play a role in disease pathogenesis. Here, we determine the spectrum and prevalence of pathogenic CaM variants in a cohort of genetically elusive LQTS, and functionally characterize the novel variants.

Methods and Results - Thirty-nine genetically elusive LQTS cases underwent whole exome sequencing to identify CaM variants. Non-synonymous CaM variants were overrepresented significantly in this heretofore LQTS cohort (15.4%) compared to exome aggregation consortium (0.04%; $p<0.0001$). When the clinical sequelae of these 6 CaM-positive cases was compared to the 33 CaM-negative cases, CaM-positive cases had a more severe phenotype with an average age of onset of 8 months, an average QTc of 679 ms, and a high prevalence of cardiac arrest. Functional characterization of one novel variant, E141G-CaM, revealed an 11-fold reduction in Ca^{2+} binding affinity and a functionally-dominant loss of inactivation in $Ca_V1.2$, mild accentuation in $Na_V1.5$ late current, but no effect on intracellular RyR2-mediated calcium release.

Conclusions - Overall, 15% of our genetically elusive LQTS cohort harbored non-synonymous variants in CaM. Genetic testing of *CALM1-3* should be pursued for individuals with LQTS, especially those with early childhood cardiac arrest, extreme QT prolongation, and a negative family history.

Key words: calmodulin; L-type calcium channels; long QT syndrome; ryanodine receptor; sodium channels

DOI: 10.1161/CIRCGENETICS.115.001323

Introduction

Calmodulin (CaM) is an essential Ca^{2+} sensing, signal-transducing protein. Calcium-induced activation of CaM regulates many calcium-dependent processes and modulates the function of cardiac ion channels including the long QT syndrome (LQTS)-associated *CACNA1C*-encoded $Ca_V1.2$ calcium channel and *SCN5A*-encoded $Na_V1.5$ sodium channel, as well as the catecholaminergic polymorphic ventricular tachycardia (CPVT)-associated *RYR2*-encoded ryanodine receptor.[1-3] Interestingly, there are three calmodulin genes, *CALM1* (chr14q31), *CALM2* (chr2p21), and *CALM3* (chr19q13),[4] with unique nucleotide sequences that all encode for a completely identical 149 amino acid CaM protein,[5, 6] which are expressed differentially in the human heart.[7]

Variants in all three of the calmodulin genes (*CALM1, CALM2,* and *CALM3)* have been described recently in LQTS.[7-9] LQTS is a disorder of ventricular myocardial repolarization characterized by the prolongation of the heart-rate corrected QT interval (QTc) on a resting electrocardiogram (ECG), manifesting clinically as syncope, seizures, or sudden death in the setting of a structurally normal heart. In 2013, whole exome sequencing (WES) was utilized on two parent-child trios of severe cases of LQTS presenting during infancy yielding de novo variants in *CALM1* and *CALM2*.[7] Follow-up cohort analysis identified two additional LQTS patients with variants in *CALM1*. Since then, additional *CALM2* variants have also been identified in cases of LQTS and LQTS/CPVT overlap phenotypes.[8] Finally, a variant was identified in *CALM3*-encoded CaM in a severe case of LQTS.[9]

All of the identified LQTS-associated variants in CaM characterized to date have reduced affinity for Ca^{2+} and attenuated $Ca_V1.2$ inactivation through the loss of calcium dependent inactivation (CDI).[7, 8, 10, 11] Here, we describe the spectrum, prevalence, and functional

consequence of novel CaM variants identified within our cohort of 39 unrelated patients with genetically elusive LQTS.

Methods

Study subjects

The study population consisted of 39 unrelated patients with clinically diagnosed LQTS with a Schwartz score ≥ 3.5 (Table 1) that were referred to the Windland Smith Rice Sudden Death Genomics Laboratory at Mayo Clinic, Rochester, MN for genetic testing. All 39 patients were genotype-negative for all known LQTS-susceptibility genes: *AKAP9, ANKB, CACNA1C, CAV3, KCNE1, KCNE2, KCNH2, KCNJ2, KCNJ5, KCNQ1, SCN4B, SCN5A*, *SNTA1,* and *TRDN*. Thus, the 39 cases tested here represent those patients that would fall within the estimated 20% remnant of patients with a clinically certain diagnosis of LQTS, yet remain without an identified genetic cause following genetic testing of all currently known LQTS susceptibility genes. This study was approved by the Mayo Foundation Institutional Review Board and informed consent was obtained for all patients.

Whole Exome Sequencing (WES) with Targeted Calmodulin Gene Analysis

All 39 LQTS patients underwent WES and subsequent calmodulin (CaM) gene (*CALM1*, *CALM2*, and *CALM3*) specific analysis. Briefly, paired-end libraries were prepared following the manufacturer's protocol (Illumina, San Diego, CA and Agilent, Santa Clara, CA) using the Bravo liquid handler from Agilent. Whole exon capture was carried out using the protocol for Agilent's SureSelect Human All Exon v4 + UTRs kit. Exome libraries were loaded onto TruSeq Rapid run paired end flow cells at concentrations of 9 pM to generate cluster densities of 600,000-800,000/mm^2 following Illumina's standard protocol using the Illumina cBot and

TruSeq Rapid Paired end cluster kit version 1. The flow cells were sequenced as 100 X 2 paired end reads on an Illumina HiSeq 2500 using TruSeq Rapid SBS kit version 1 and HiSeq data collection version 2.0.12.0 software. Base-calling was performed using Illumina's RTA version 1.17.21.3.

The Illumina paired end reads were aligned to the hg19 reference genome using Novoalign 2.08 (http://novocraft.com) followed by the sorting and marking of duplicate reads using Picard (http://picard.sourceforge.net). Local realignment of INDELs and base quality score recalibration were then performed using the Genome Analysis Toolkit 2.7-4 (GATK).[12] Single nucleotide variants (SNVs) and insertions/deletions (INDELs) were called across all of the samples simultaneously using GATK's Unified Genotyper with variant quality score recalibration.[13]

Following the Mayo Clinic bioinformatics pipeline analysis, the data was provided in comprehensive Microsoft Excel (Redmond, WA) spreadsheet with all of the identified variants across WES samples. Using filter functions in Microsoft Excel, we searched for variants within *CALM1* (NM_006888), *CALM2* (NM_001743), and *CALM3* (NM_005184) that had a genotype call quality score of > 20 and a read depth of > 10. To be considered as a putative pathogenic variant, the identified CaM variants had to be i) non-synonymous (amino acid altering), ii) involve a highly conserved amino acid, iii) and absent in the Exome Aggregation Consortium (ExAC , n=60,706) database.[14] All CaM variants identified through WES were Sanger sequence verified. Primer sequences and conditions are available upon request.

Functional Analysis

The novel CaM variant (p.E141G) was characterized functionally using Ca^{2+} binding assays and patch-clamp electrophysiological recording to assess its pathogenicity.

Generation of recombinant CaM and measurement of Ca^{2+} binding to CaM

Wildtype and mutant CaM proteins were prepared and the Ca^{2+} affinities for WT- and E141G-CaM were determined using methods previously described.[7]

CaM mammalian expression vectors and site-directed mutagenesis

The EGFP-HA-CaM (EGFP: enhanced green florescent protein) vector, kindly provided by Dr. Emanuel Strehler, Mayo Clinic, Rochester, MN, was used for the heterologous expression electrophysiology studies of $Ca_V1.2$ and $Na_V1.5$ in TSA201 cells. The p.E141G missense variant was engineered into EGFP-HA-CaM vector using primers containing the missense variant (available upon request) in combination with the Quikchange II XL Site-Directed Mutagenesis Kit (Stratagene, La Jolla, CA). The integrity of all constructs was verified by DNA sequencing.

Heterologous expression and electrophysiological analysis of $Ca_V1.2$ co-expressed with WT- or E141G-CaM

The constructs utilized to recapitulate $Ca_V1.2$ have been described previously.[15] TSA201 cells were cultured in Dulbecco's Modification of Eagle's Medium supplemented with 10% Fetal Bovine Serum (FBS), 1.0% L-glutamine, and 1.2% penicillin/streptomycin solution in a 5% CO_2 incubator at 37°C. Heterologous expression of $Ca_V1.2$ was accomplished by co-transfecting 1 μg *CACNA1C* ([(EYFP)Nα1c,77] in pcDNA),[15] 1 μg *CACNB2b* (in pIRES2-dsRED2),[15] and 1 μg *CACNA2D1* (in pcDNA3.1)[15] vectors with either 0.5 μg a green fluorescent protein empty vector (GFP-EV; kindly provided by Dr. Gianrico Farrugia, Mayo Clinic, Rochester MN), EGFP-HA-CaM-WT, or EGFP-HA-CaM-E141G vectors using 9 μl Lipofectamine 2000 (Invitrogen, Carlsbad, CA). The media was replaced with fresh OPTI-MEM after 4-6 hours. Transfected TSA201 cells were cultured in OPTI-MEM and incubated for 48 hours and cells exhibiting green, red, and yellow fluorescence were selected for electrophysiological experiments. Standard

whole-cell patch clamp technique was used to measure $Ca_V1.2$ WT currents co-expressed with WT- or E141G-CaM at room temperature (22-24 ^oC) as described previously.[15] In addition, we also examined persistent I_{CaL} current, which was measured at the end of a 500 ms long depolarization.

Animal use and experiments in ventricular myocytes

The use of animals in this study was approved by the Animal Care and Use Committees of Vanderbilt University, Nashville, TN, USA and performed in accordance with National Institutes of Health guidelines. Single ventricular myocytes from 10- to 16-week-old C57BL/6 mice were isolated by enzymatic digestion using collagenase as previously described.[16] Inactivation of $Ca_V1.2$ current was studied in freshly isolated murine ventricular myocytes using whole-cell patch clamp technique. CaM (total concentration 6 μM for all experiments) was added to pipette solution and then dialyzed into the cell via patch pipette. Currents were elicited with 500-ms depolarizing pulses to 0 mV from holding potential (HP) of -70 mV applied every 2 minutes to track the effect of CaM over time, as it diffuses into the cell. Usually, the effect of CaM on inactivation reached its maximum 4-6 min after start of dialysis. 15-ms pre-pulses to -40 mV were applied prior to the test pulse to inactivate Na^+ currents. Cells were pre-treated with ryanodine (50 μM) and thapsigargin (10 μM) for 30 min prior to experiment to prevent sarcoplasmic reticulum (SR) Ca^{2+} release. Experiments were conducted at room temperature. For mixing studies, a mixture of 75% of WT CaM and 25% of mutant CaM (total CaM concentration 6 μM) was used. Tau values represent mono-exponential fit of the last 350 ms of the current during depolarizing step.

In addition, Ca^{2+} spark measurements to examine RyR2 activity were completed as previously described.[3]

Heterologous expression and electrophysiological analysis of $Na_V1.5$ co-expressed with WT- or E141G-CaM

In order to recapitulate the *SCN5A*-encoded $Na_V1.5$ sodium channel, 1 μg of the human cardiac voltage-dependent Na^+ channel α subunit (H558/Q1077del, Genbank accession no.AY148488) in the pcDNA3 vector (Invitrogen, Carlsbad, CA) was co-transfected with either 0.5 μg GFP-EV, EGFP-HA-CaM-WT, EGFP-HA-CaM-E141G, or 0.25 μg EGFP-HA-CaM-WT + 0.25 μg EGFP-HA-CaM-E141G with the use of 4μl Lipofectamine in TSA201 cells. Transfected TSA201 cells were cultured in OPTI-MEM (Gibco, Carlsbad, CA) and incubated for 24 hours after transfection and cells exhibiting green fluorescence were selected for electrophysiological experiments. Standard whole-cell patch clamp technique was used to measure $Na_V1.5$ WT currents co-expressed with WT-CaM, E141G-CaM, or WT-CaM + E141G-CaM (to mimic the heterozygous state of the patient) at room temperature as previously described.[17] Late I_{Na} was measured at the end of 700 ms long depolarization.

Statistical analysis

Data are presented as mean values ± standard error of the mean (SEM) or ± 95% confidence intervals. Comparisons were made using one-way ANOVA or Student's t-test where appropriate and p-values < 0.05 were considered significant. Chi square test with Yates correction was utilized to derive the p-value to test for the enrichment of variants in the 39 variants versus ExAC.[14] Categorical comparisons were made using a Fisher's exact test and p-values < 0.05 were considered significant.

Results

Genetic Analysis

Our genetically elusive LQTS cohort consisted of 39 individuals (41% males, average age at

diagnosis was 20 ± 18 years, 26% were < 5 years-old). The average QTc was 538 ± 13 ms, 38% experienced syncope, 36% cardiac arrest, and 36% had a positive family history of cardiac arrhythmias or sudden unexplained death (Table 1).

WES revealed 6 CaM missense variants, p.D96V (c.287 A>T, *CALM2*), p.D130G (c.389 A>G, *CALM2*), p.D130V (c.389 A>T, *CALM2*), p.E141G (c.422 A>G, *CALM1*), and two cases with p.F142L (c.426 C>G, *CALM1*), in a total of 6 of 39 cases (15.4%; Table 2, Figure 1). Both p.D130V and p.E141G represent novel CaM variants. The, p.D96V, p.D130G, and p.F142L CaM variants have been characterized functionally and described previously as LQTS-susceptibility variants (Table 2).[7, 10, 11, 18] Our previously discovered *CALM3*-variant positive child was not included in this cohort of unrelated cases as the child's variant had been discovered by WES and genomic triangulation (proband/parent trio) akin to the previous *CALM1* and *CALM2* discoveries.[9]

The p.D96V variant was identified in a female who was diagnosed prenatally with LQTS (Figure 1). She was delivered at term and her first ECG demonstrated a QTc of 690 ms, 2:1 AV block, and T-wave alternans (TWA). She was treated with beta-blockers and discharged. At 1-month of age, she experienced her first sudden cardiac arrest (SCA), and a single chamber internal cardiac defibrillator (ICD) was implanted. She developed a brain injury from the SCA and at 2-years-old developed seizures as a result. The family history was negative for arrhythmias and sudden death. Parental DNA was unavailable to test for de novo versus familial inheritance of the variant.

The p.D130G variant was identified in a female born at term that was noted to have bradycardia (Figure 1). An ECG, recorded 12 hours after birth, revealed a QTc of 740 ms and 2:1 AV block. She was treated with beta-blockers, phenytoin, spironolactone, potassium, and a

single chamber pacemaker in the first week of life. At 6-years-old, a single chamber ICD was implanted and beta-blocker therapy continued. At 11- and 14-years-old, she experienced appropriate ICD discharges for ventricular fibrillation (VF). The family history was negative. Parental DNA was unavailable.

The p.D130V variant was identified in a male born with 2:1 AV block in utero (Figure 1). QT prolongation (QTc = 800 ms) was documented at birth, macroscopic TWA was observed, and beta-blocker therapy was initiated. Echocardiograms at the first month of life showed restrictive cardiomyopathy with borderline systolic function. In his second month of life, he developed torsades de pointes, and subsequently had a left T2-T4 sympathetic denervation and minimally invasive epicardial ICD. His beta-blocker was combined with sodium channel blockers. At 6-years-old he experienced an appropriate VF-terminating shock after a medication dose change by his parents. His echocardiograms demonstrated dilated cardiomyopathy with hypertrabeculation, and continued QT prolongation. At 7-years-old, he had an additional VF-terminating shock after missing a single beta-blocker dose. The family history was negative. The p.D130V was absent in both parents, thus confirming a de novo occurrence in the child.

The p.E141G variant was identified in a male with his first unwitnessed syncopal event at 3 years of age from which he was found unconscious and spontaneously recovered (Figure 1). He experienced his first SCA at 4 years of age in which CPR was initiated, and after 30 minutes, consciousness was regained. After his SCA, an ECG revealed a QTc of 610 ms, and he was treated subsequently with beta blockers and sodium channel blockers. His QT prolongation has persisted, however the index case is now 11-years-old and has not experienced an episode since the initiation of treatment. An echocardiogram revealed mild LV dilation; however the cardiac valves and structure were normal. In addition, it was noted that he has speech and motor skill

delay. He has negative family history. The p.E141G was not identified in either parent confirming a de novo occurrence in the child.

The p.F142L variant was identified in a female. Her ECG shortly after birth showed a QTc of 612 ms and 2:1 AV block (Figure 1). Her initial treatment consisted of beta-blockers and at 19 months a dual chamber pacemaker was implanted. Shortly thereafter, she had SCA, which caused anoxic brain injury and seizure-like syncopal episodes. After the initiation of this genetic investigation, the patient died suddenly. She was brought to the emergency room for altered mental status. Echocardiogram revealed severely diminished left ventricular systolic dysfunction. Soon after arrival she deteriorated to ventricular fibrillation and was unable to be resuscitated. Her autopsy revealed cardiomegaly with dilation and hypertrophy. She had no family history of arrhythmias, and her mother was negative for the p.F142L variant. The father's sample was unavailable.

This p.F142L variant was also identified in a male. He was delivered at term, and bradycardia was noted. This prompted an ECG which revealed a QTc of 620 ms. He was treated with beta-blockers and had a pacemaker placed for atrial pacing. This combination therapy was associated with an attenuation of his QTc down to 540 ms. Shortly after recruitment into our study at 1 year and 3 months of age, this patient died suddenly. He was placed for a nap and was found gasping for air, unconscious and blue, and unfortunately was unable to be resuscitated. Interrogation of his pacemaker showed sinus rhythm with 1:1 conduction just before a period of fast VF which stabilized into VT. He had no prior recorded events on his pacemaker. ECGs were obtained for the parents and siblings, all were normal, and both parents were negative for the p.F142L variant, supporting de novo occurrence.

Over-representation of CaM variants in LQTS versus ExAC

Non-synonymous CaM variants were overrepresented significantly in our LQTS cohort (6/39; 15.4%) compared to ExAC (23/60,706; 0.04%, p<0.0001; Figure 1). The 21 rare non-synonymous CaM variants identified in ExAC are shown in Figure 1 and Supplemental Table 1. Interestingly, all 8 of the pathogenic CaM residues (D96, N98, D130, D132, D134, Q136, E141, and F142)[7-9] that are affected in LQTS patients reside within one of the four EF-hands, where Ca^{2+} binds to CaM. Specifically, these pathogenic variants localize to either the third (D96 and N98) or fourth (D130, D134, Q136, E141, and F142) EF-hands located in the C-domain (Figure 1). Moreover, the side chains of 7 of these 8 residues interact directly with Ca^{2+}. In contrast, only 4 of the 21 unique variants in ExAC (G24, I28, A103, and A104) reside within an EF-hand calcium binding loop, however none of them involve a residue whose side chain interacts directly with calcium (Figure 1). In addition, there are two extremely rare protein truncating variants (G42* and D51Gfs*5) present in the ExAC browser that were identified in 2/60,706 individuals. However, given the severity of CaM-related LQTS, this would suggest that having a non-functioning CaM protein from one of six CaM-generating alleles is not pathogenic.[14]

Demographic and clinical characteristics of patients harboring CaM variants

Compared to our original LQTS referral cohort that comprised 541 patients in 2005 where the average age at diagnosis was 24 ± 16 years, the average QTc was 482 ± 57 ms, and 12% had cardiac arrest,[19] Table 3 details the differences between LQT1-3 positive and LQT1-3 negative cases in this original cohort,[19] the CaM-positive cases herein, and the CaM-negative cases that still remain genetically elusive. The average age of CaM-positive patients was significantly younger (0.67 years) compared to CaM-negative (23 years; p<0.01; Figure 2A; Table 3).[19] In addition, the yield of CaM variants was significantly higher in patients < 5-years-old (6/10, 60%)

compared to patients ≥ 5 years-old (0/29, 0%, p<0.0001; Figure 2B). The average QTc was significantly longer in CaM- positive patients (679 ± 32 ms) compared to CaM-negative patients (514 ± 9 ms; p<0.0001; Figure 2C; Table 3).[19] In addition, the occurrence of cardiac arrest was significantly higher in CaM-positive patients (6/6; 100%) compared to CaM-negative patients (8/33; 24%, p<0.001; Figure 2D; Table 3).[19]

Functional Characterization

Since p.D96V, p.D130G, and p.F142L are disruptive functionally (Table 2),[7, 10, 11] we confidently conclude that these variants are responsible for the LQTS phenotype observed in our patients. Although p.D130V is novel, we believe that because glycine (G) and valine (V) are replacing a critical negatively charged aspartic acid (D) known to interact with the positively charged calcium ion (Figure 1), p.D130V will functionally and clinically mimic p.D130G. The p.E141G variant was the only variant affecting a novel residue and we therefore characterized it functionally in this study.

E141G-CaM impairs Ca^{2+} binding by CaM

In line with previous observations, the p.E141G variant, located in EF-hand IV of the C-domain (Figure 1), decreased the Ca^{2+} affinity of the C-domain (by 11-fold) but did not significantly alter the Ca^{2+} affinity of the N-domain (Figure 3A).

E141G-CaM disrupts $Ca_V1.2$'s CDI

The previously published LQTS-associated CaM variants significantly impaired $Ca_V1.2$ calcium dependent inactivation (CDI) leading to a loss of inactivation.[11, 10] Therefore, we examined the effects of p.E141G-CaM on $Ca_V1.2$ in a heterologous expression system. Typical $Ca_V1.2$ tracings of voltage-dependent activation from $Ca_V1.2$ with GFP-EV, WT- and E141G-CaM are shown in Figure 3B with holding potential at -90 mV to various depolarization potentials (see

figure legend). Current-voltage relationship shows that p.E141G-CaM did not change $Ca_V1.2$ peak current density (Figure 3C). However, p.E141G-CaM shifted $Ca_V1.2$ $V_{1/2}$ of steady-state inactivation 1.9 mV from -16.8 ± 0.23 mV ($Ca_V1.2$+WT-CaM; n=11) to -14.9 ± 0.27 mV ($Ca_V1.2$+E141G-CaM; n=9). The p.E141G-CaM also shifted $Ca_V1.2$ $V_{1/2}$ of activation -3.9 mV from 16.4 ± 0.97 mV ($Ca_V1.2$+WT-CaM, n=12) to 12.5 ± 0.76 mV ($Ca_V1.2$+E141G-CaM; n=12; $p < 0.05$; Figure 3D).

$Ca_V1.2$+E141G-CaM exhibited much slower fast and slow decay time across the voltages +10 mV to +50 mV compared with $Ca_V1.2$+WT-CaM (n=10 for each group, $p<0.05$) (Figure 3E-F). Typical $Ca_V1.2$ current tracings from $Ca_V1.2$+EV, WT-CaM, and E141G-CaM are shown in Figure 4A**.** E141G-CaM increased $Ca_V1.2$'s persistent current 7.1 fold from 2.1 ± 0.5% ($Ca_V1.2$ + WT-CaM; n=9) to 17.0 ± 3.0% ($Ca_V1.2$ + E141G-CaM; n=10, $p<0.05$; Figure 4B).

We next tested the effect of E141G-CaM in native murine ventricular myocytes. As in our heterologous expression system, E141G-CaM drastically impaired $Ca_V1.2$ current inactivation without affecting peak currents (Figure 4C-E). Even a 25% fraction of E141G-CaM in the presence of 75% WT-CaM was sufficient to significantly impair the $Ca_V1.2$ inactivation, which is consistent with a dominant negative effect.

E141G-CaM accentuates $Na_V1.5$ late current

Next, we determined if E141G-CaM affected the electrophysiological characteristics of $Na_V1.5$. Typical I_{Na} tracings of voltage-dependent activation from $Na_V1.5$ with GFP-EV, WT- and E141G-CaM are shown in Figure 5A with holding potential at -100 mV to various depolarization potentials (see figure legend). Current-voltage relationship shows that WT- and E141G-CaM did not change $Na_V1.5$ peak current density, voltage-dependent inactivation or activation, or decay time (Figure 5B-D).

Typical $Na_V1.5$ late current tracings from $Na_V1.5$ with EV, WT-, E141G-CaM, and WT-CaM+E141G-CaM are shown in Figure 5E. E141G-CaM increased $Na_V1.5$'s late current 1.7-fold from 0.13 ± 0.01% ($Na_V1.5$+WT-CaM; n=8) to 0.35 ± 0.06% ($Na_V1.5$+E141G-CaM; n=10; $p<0.05$; Figure 5F). However, when WT-CaM was co-expressed with E141G-CaM, there was no longer an effect on the $Na_V1.5$ peak late current (Figure 5E-F). This result suggests that unlike for Cav1.2, there was no functional dominance of E141G-CaM in the regulation of $Na_V1.5$ late currents.

E141G-CaM has no effect on RyR2 Ca^{2+} release channels and SR Ca^{2+} handling

CaM variants have also been identified in patients with CPVT,[18] leading to activation of RyR2 SR Ca^{2+} release channels.[3] However, to date, the known LQTS-associated CaM variants have exerted no effect or only slightly reduced RyR2 Ca^{2+} release channel activity.[20] Therefore, we determined the effect of E141G-CaM on intracellular Ca^{2+} handling by measuring Ca^{2+} sparks (a measure of RyR2 Ca^{2+} release channel activity) and found that E141G-CaM had no effect on Ca^{2+} sparks and SR Ca^{2+} content (Figure 6).

Discussion

Our examination of 39 patients with genetically elusive LQTS identified 6 individuals (15.4%) that harbored variants in either *CALM1* or *CALM2*. Three of the identified variants, p.D96V, p.D130G, and p.F142L, had been published previously in other cases of LQTS,[7] one variant represented a novel amino acid change at a previously described position, p.D130V, and the final variant, p.E141G, was novel. Within our cohort, CaM variants were overrepresented significantly when compared to the publically available databases in essentially a modified case:control analysis, which provides additional evidence that single amino acid substitutions

within CaM, particularly those involving calcium-interacting residues in the C-domain, are not well tolerated.

When examining the clinical characteristics of these six patients harboring CaM variants, we found that they had an early age at onset with the average age of onset at 8 months, average QTc of 679 ± 32 ms, and all experienced cardiac arrest (Figure 2, Table 3).[19] Moreover, all CaM variants were shown to occur as de novo when parental DNA was available for testing, thus supporting the malignant nature of LQTS-related CaM variants. These clinical characteristics seemed even more severe than those of the previously published LQT1-3 genotype-positive and LQT1-3 genotype-negative LQTS (Table 3),[19] and the previously described LQTS[7] and LQTS/CPVT[8] patients with CaM variants (n=10), where the average age at diagnosis was 3 years, the average QTc was 591 ± 22 ms, and 60% experienced cardiac arrest (Table 2). However, if we separate the previously described CaM-positive patients into two categories, LQTS/CPVT overlap phenotypes and a pure LQTS phenotype, it becomes more apparent that LQTS/CPVT patients (n=3)[8] may be less severe, as the average age at diagnosis was 7 years, the average QTc was 519 ± 53 ms, with only 33% experiencing cardiac arrest. In contrast, the patients with a pure LQTS phenotype (n=7) were similar to our LQTS CaM-positive patients, with an average age at diagnosis of 14 months, an average QTc of 622 ± 20 ms, and with 86% experiencing cardiac arrest. This provides evidence that CaM-mediated LQTS is very severe and it may be important to delineate these phenotypes, as they may present with different disease severities, and the phenotypic presentation may be regulated by distinct underlying mechanisms. Therefore, continued studies will be necessary to elucidate the key differences between CaM variants and their associated phenotypes. In addition, children with CaM-mediated LQTS who survive will need ongoing surveillance for the potential development of a cardiomyopathy as two

of the CaM variant-positive children who have survived past 5 years of age, and one of the deceased patients on autopsy, had developed dilated cardiomyopathy. It is possible that the $Ca_V1.2$'s impaired CDI may contribute to diastolic calcium excess that could precipitate cardiomyopathic structural remodeling.

CaM modulates the activity of several different ion channels by sensing and transducing Ca^{2+} signals. When Ca^{2+} levels are raised, CaM binds up to 4 calcium ions, which stabilize an open conformation within each domain that mediates interactions with CaM's targets. Hence, we first examined the effects of the E141G variant on the Ca^{2+} affinity of CaM, and found that this mutant resulted in an 11-fold reduction in the Ca^{2+} affinity of the C-domain. These results are comparable to the Ca^{2+} binding impairments caused by the 8 variants previously associated with LQTS or LQTS/CPVT overlap phenotypes (5-54 fold increased dissociation of Ca^{2+} in the C-domain, Table 2), [7, 10, 18] suggesting that impaired Ca^{2+} binding properties in the C-domain is a common underlying pathomechanism of LQTS-associated CaM variants.

These disrupted Ca^{2+} affinities have direct implications on $Ca_V1.2$'s CDI. Typically, $Ca_V1.2$ is inactivated with increasing Ca^{2+} concentrations via a mechanism mediated by the binding of CaM. The altered Ca^{2+} binding properties of CaM, such as with CaM-E141G, would therefore be expected to impair $Ca_V1.2$'s CDI. Using whole-cell patch clamp experiments, we found that CaM-E141G shifted inactivation 1.9 mV. These findings were replicated in native ventricular myocytes where CaM-E141G again reduced $Ca_V1.2$ inactivation, which closely parallels what has been noted previously with the other LQTS-associated CaM variants.[10, 11]

Because there are three calmodulin genes expressed in the heart, which each encode for an identical protein, our heterozygous variant only affects 1/6 of the calmodulin alleles. Therefore, we examined the CaM-E141G variant at reduced levels (25:75; mutant:WT), which

also maintained a significant effect on inactivation. This suggests that p.E141G has a dominant negative effect and is capable of causing the disease phenotype.

In addition to $Ca_V1.2$, it has been established previously that CaM modulates cardiac sodium channel inactivation.[21] Previously, Yin and colleagues found that LQTS-associated CaM variants (D96V, D130G, and F142L) did not affect $Na_V1.5$; however D130G led to a 7.5-fold increase in fetal $Na_V1.5$ late current.[11] They hypothesized that because CaM-mediated LQTS has an early age of onset, the variants may only affect the fetal isoform of the sodium channel. However, because there have been associations of CaM with the adult isoform of $Na_V1.5$, we wanted to determine whether CaM-E141G may have an effect on channel gating function. Our studies showed that the E141G variant led to a 1.7-fold increase in $Na_V1.5$ late current when expressed as a homozygote. This makes our CaM-E141G variant the first CaM variant shown to affect the adult isoform of the cardiac sodium channel. Interestingly, however, when E141G was expressed with wild-type CaM – mimicking a heterozygote patient – the $Na_V1.5$ late current was normalized. This differs from the effect of E141G-CaM on $Ca_V1.2$, where even a 3-fold excess of WT CaM failed to normalize $Ca_V1.2$ inactivation.

It has been established that CPVT-associated CaM variants[18] affect the functioning of *RYR2*- encoded ryanodine receptor (RyR2), leading to greater open probability of the channel.[3] Because one previously reported LQTS associated CaM variant (N98S) also activates RyR2 and can cause CPVT as well as LQTS,[3] we examined the effect of p.E141G on RyR2 Ca^{2+} release channel activity. The p.E141G variant had no effect on Ca^{2+} sparks, a measure of RyR2 Ca^{2+} release channel activity, and did not affect SR Ca^{2+} content. Hence, our results continue to support the emerging evidence that LQTS-associated CaM variants do not affect RyR2, whereas CPVT-associated CaM variants perturb RyR2 function.

DOI: 10.1161/CIRCGENETICS.115.001323

Conclusion

We have identified a novel CaM variant p.E141G, which like other LQTS-associated CaM variants, disrupts Ca^{2+} binding and leads to increased $Ca_V1.2$ window/persistent current. In addition, p.E141G is the first CaM variant identified to also affect the adult $Na_V1.5$ isoform, leading to increased sodium late current. Overall, we found that 15% of genetically elusive LQTS patients harbored a functionally significant CaM variant. The phenotypic characteristics of the CaM-positive individuals from our cohort, combined with the other published cases of LQTS-associated CaM variants, suggest that LQTS patients harboring variants in either *CALM1-, CALM2-,* or *CALM3*-encoded CaM present early in life with profound QT prolongation and have a high predilection for cardiac arrest and sudden death. The existing gene panels for LQTS genetic testing should now be expanded to include *CALM1, CALM2,* and *CALM3.*

Acknowledgments: We would like to acknowledge gratefully Dr. Emanuel Strehler at the Mayo Clinic for sharing his expertise of the calmodulins and for sharing his calmodulin DNA constructs.

Funding Sources: This work was supported by the Mayo Clinic Windland Smith Rice Comprehensive Sudden Cardiac Death Program, the Sheikh Zayed Saif Mohammed Al Nahyan Fund in Pediatric Cardiology Research, the Dr. Scholl Fund, and the Hannah M. Wernke Memorial Fund. This project was also supported in part by funding from Mayo Clinic's Center for Individualized Medicine (CIM). CNJ was supported by fellowships from the American Heart Association (13POST14380036) and the National Institutes of Health (5 F32 HL117612-02). Research on calcium binding proteins in the Chazin laboratory is supported by an endowed chair. This work was also partly supported by the United States National Institutes of Health (HL88635, HL71670 & HL124935 to BCK)

Conflict of Interest Disclosures: MJA is a consultant for Boston Scientific, Gilead Sciences, Medtronic, and St. Jude Medical. In addition, MJA, DJT, and Mayo Clinic receive sales based royalties from Transgenomic for their FAMILION-LQTS and FAMILION-CPVT genetic tests. However, none of these entities contributed to this study in any manner. NJB, NGH, DY, MLC, DK, HSH, CNJ, WJC, CGL, MS, ALP, YRL, RK and BCK have no conflicts of interest.

References:

1. Levitan IB. It is calmodulin after all! Mediator of the calcium modulation of multiple ion channels. *Neuron*. 1999;22:645-648.

2. Gabelli SB, Boto A, Kuhns VH, Bianchet MA, Farinelli F, Aripirala S, Yet al. Regulation of the Nav1.5 cytoplasmic domain by calmodulin. *Nat Commun*. 2014;5:5126.

3. Hwang HS, Nitu FR, Yang Y, Walweel K, Pereira L, Johnson CN, et al. Divergent regulation of ryanodine receptor 2 calcium release channels by arrhythmogenic human calmodulin missense mutants. *Circ Res*. 2014;114:1114-1124.

4. Berchtold M, Egli R, Rhyner J, Hameister H, Strehler E. Localization of the human bona fide calmodulin genes calm1, calm2, and calm3 to chromosomes 14q24-q31, 2p21.1-p21.3, and 19q13.2-q13.3. *Genomics*. 1993;16:461-465.

5. Fischer R, Koller M, Flura M, Mathews S, Strehler-Page M, Krebs J, et al. Multiple divergent mrnas code for a single human calmodulin. *J Biol Chem*. 1998;263:17055-17062.

6. SenGupta B, Friedberg F, Detera-Wadleigh S. Molecular analysis of human and rat calmodulin complementary DNA clones. Evidence for additional active genes in these species. *J Biol Chem*. 1987;262:16663-16670.

7. Crotti L, Johnson CN, Graf E, De Ferrari GM, Cuneo BF, Ovadia M, et al. Calmodulin mutations associated with recurrent cardiac arrest in infants. *Circulation.* 2013;127:1009-1017.

8. Makita N, Yagihara N, Crotti L, Johnson CN, Beckmann BM, Roh MS, et al. Novel calmodulin mutations associated with congenital arrhythmia susceptibility. *Circ Cardiovasc Genet*. 2014;7:466-474.

9. Reed GJ, Boczek NJ, Etheridge SP, Ackerman MJ. CALM3 mutation associated with long QT syndrome. *Heart Rhythm*. 2015;12:419-422.

10. Limpitikul WB, Dick IE, Joshi-Mukherjee R, Overgaard MT, George AL, Jr., Yue DT. Calmodulin mutations associated with long qt syndrome prevent inactivation of cardiac l-type ca(2+) currents and promote proarrhythmic behavior in ventricular myocytes. *J Mol Cell Cardiol.* 2014;74:115-124.

11. Yin G, Hassan F, Haroun AR, Murphy LL, Crotti L, Schwartz PJ, et al. Arrhythmogenic calmodulin mutations disrupt intracellular cardiomyocyte Ca2+ regulation by distinct mechanisms. *J Am Heart Assoc*. 2014;3:e000996.

12. McKenna A, Hanna M, Banks E, Sivachenko A, Cibulskis K, Kernytsky A, et al. The genome analysis toolkit: A mapreduce framework for analyzing next-generation DNA sequencing data. *Genome Res.* 2010;20:1297-1303.

13. DePristo MA, Banks E, Poplin R, Garimella KV, Maguire JR, Hartl C, Pet al. A framework for variation discovery and genotyping using next-generation DNA sequencing data. *Nat Genet*. 2011;43:491-498.

14. Exome aggregation consortium (exac), cambridge, ma (url: Http://exac.Broadinstitute.Org) [date (November, 2015) accessed].

15. Boczek NJ, Miller EM, Ye D, Nesterenko VV, Tester DJ, Antzelevitch C, et al. Novel timothy syndrome mutation leading to increase in cacna1c window current. *Heart Rhythm.* 2015;12:211-219.

16. Knollmann BC, Chopra N, Hlaing T, Akin B, Yang T, Ettensohn K, et al. Casq2 deletion causes sarcoplasmic reticulum volume increase, premature Ca2+ release, and catecholaminergic polymorphic ventricular tachycardia. *J Clin Invest*. 2006;116:2510-2520.

17. Van Norstrand DW, Valdivia CR, Tester DJ, Ueda K, London B, Makielski JC, et al. Molecular and functional characterization of novel glycerol-3-phosphate dehydrogenase 1 like gene (GPD1-L) mutations in sudden infant death syndrome. *Circulation*. 2007;116:2253-2259.

18. Nyegaard M, Overgaard Michael T, Sondergaard Mads T, Vranas M, Behr Elijah R, Hildebrandt Lasse L, et al. Mutations in calmodulin cause ventricular tachycardia and sudden cardiac death. *Am J Hum Genet*. 2012;91:703-712.

19. Tester DJ, Will ML, Haglund CM, Ackerman MJ. Compendium of cardiac channel mutations in 541 consecutive unrelated patients referred for long qt syndrome genetic testing. *Heart Rhythm*. 2005;2:507-517.

20. Watanabe H, Knollmann BC. Mechanism underlying catecholaminergic polymorphic ventricular tachycardia and approaches to therapy. *J Electrocardiol*. 2011;44:650-655.

21. George AL, Jr. Inherited disorders of voltage-gated sodium channels. *J Clin Invest.* 2005;115:1990-1999.

DOI: 10.1161/CIRCGENETICS.115.001323

Table 1: Demographics of our genotype negative LQTS cohort

Number of Probands	39
Age at Diagnosis, years ± SD	20 ± 18
Range	0-65
< 5 years of age (%)	10 (26)
≥ 5 years of age (%)	29 (74)
Males (%)	16 (41)
QTc, ms ± SEM	538 ± 13
Syncope (%)	15 (38)
Cardiac Arrest (%)	14 (36)
Positive Family History (%)	14 (36)

DOI: 10.1161/CIRCGENETICS.115.001323

Table 2: CaM Variants in LQTS and LQTS/CPVT Overlap Phenotypes.

Study	Variants	Gene	Disease	Sex	Race	QTc (ms)	Age at diagnosis	Events	Increased Ca^{2+} Dissociation C-Domain	$Ca_V1.2$	$Na_V1.5$	RyR2
Crotti	p.D96V	*CALM2*	LQTS	F	Hispanic	690	prenatal	Cardiac arrest	14-fold	Loss of CDI	No effect	No effect
Boczek	**p.D96V**	***CALM2***	**LQTS**	**F**	**Hispanic**	**690**	**prenatal**	**Cardiac arrest**	**14-fold**	**Loss of CDI**	**No effect**	**No effect**
Makita	p.N98I	*CALM2*	LQTS	M	White – England	555	17 months	Cardiac arrest	7-fold	NA	NA	NA
Makita/ Nyegaard	p.N98S	*CALM2*	LQTS/ CPVT	M	Japanese	478	5 years	Syncope during exertion	1.7-fold decreased affinity	1.6-fold decrease in CDI	NA	Greater open probability
Crotti	p.D130G	*CALM1*	LQTS	F	White – Italy	630	6 months	Cardiac arrest	54-fold	Loss of CDI	7.5-fold increase in fetal $Na_V1.5$ late current	Lower binding affinity
Crotti	p.D130G	*CALM1*	LQTS	M	Grecian	610	1 month	Cardiac arrest	54-fold	Loss of CDI	7.5-fold increase in fetal $Na_V1.5$ late current	Lower binding affinity
Reed	p.D130G	*CALM3*	LQTS	M	White	690	birth	None	54-fold	Loss of CDI	7.5-fold increase in fetal $Na_V1.5$ late current	Lower binding affinity
Boczek	**p.D130G**	***CALM2***	**LQTS**	**F**	**Indian**	**740**	**birth**	**Cardiac arrest**	**54-fold**	**Loss of CDI**	**7.5-fold increase in fetal $Na_V1.5$ late current**	**Lower binding affinity**
Boczek	**p.D130V**	***CALM2***	**LQTS**	**M**	**White**	**800**	**birth**	**Cardiac arrest**	**NA**	**NA**	**NA**	**NA**
Makita	p.D132E	*CALM2*	LQTS/ CPVT	F	White – Germany	578	<9 years	Exercise induced syncope	23-fold	NA	NA	NA
Makita	p.D134H	*CALM2*	LQTS	F	Japanese	579	6 years	Cardiac arrest	13-fold	NA	NA	NA
Makita	p.Q136P	*CALM2*	LQTS/ CPVT	F	Morracan	500	8 years	Syncope – SCD age 11	9-fold	NA	NA	NA
Boczek	**p.E141G**	***CALM1***	**LQTS**	**M**	**Indian**	**610**	**4 years**	**Cardiac arrest**	**11-fold decreased affinity**	**8.1-fold increase in $Ca_V1.2$ late current**	**2.7-fold increase in $Na_V1.5$ late current**	**No effect**
Crotti	p.F142L	*CALM1*	LQTS	F	White – Italy	600	prenatal?	Cardiac arrest	5-fold	Yes – loss of CDI	No effect	Lower binding affinity
Boczek	**p.F142L**	***CALM1***	**LQTS**	**F**	**Black**	**612**	**birth**	**Cardiac arrest – SCD 2**	**5-fold**	**Yes – loss of CDI**	**No effect**	**Lower binding affinity**
Boczek	**p.F142L**	***CALM1***	**LQTS**	**M**	**Hispanic**	**620**	**birth**	**SCD – 1 year**	**5-fold**	**Yes – loss of CDI**	**No effect**	**Lower binding affinity**

Bold represents CaM positive individuals identified in our cohort of 39 LQTS patients.[3, 7-11, 18]
NA represents when the test has not been performed
SCD stands for sudden cardiac death

Table 3: Demographics of CaM-positive, CaM-negative compared to a previously published cohort of 541 cases of LQTS

	CaM-Positive (n=6)	CaM-Negative (n=33)	LQT1-3 Positive[19] (n=272)*	LQT1-3 Negative[19] (n=269)†
Male/Female	3/3	13/20	94/178	89/180
Age at Diagnosis years ± SD	0.67 ± 2	23 ± 18	23 ± 16	25 ± 16
QTc, ms ± SEM	679 ± 32	514 ± 9	494 ± 51	470 ± 60
Cardiac Arrest (%)	100	29	13	12

*LQT1-3 Positive represents individuals who were positive for putative pathogenic variants in *KCNQ1, KCNH2,* or *SCN5A* from a larger cohort of 541 unrelated individuals with LQTS from a previously published study.[19]

†LQT1-3 Negative represents individuals who were negative for putative pathogenic variants in *KCNQ1, KCNH2,* or *SCN5A* from a larger cohort of 541 unrelated individuals with LQT from a previously published study.[19]

Figure Legends:

Figure 1: CaM variants identified in individuals with LQTS and the publically available databases. On the right is a schematic rendering of the CaM protein highlighting the N-domain and C-domain, each containing two EF hands (labeled EF-I through EF-IV) with Ca^{2+} (pink) bound. White circles represent the WT residues, red circles represent the variant residues found

in our LQTS cohort, black circles represented previously published CaM variants in LQTS, grey circles represent variant residues found in all three CaM proteins in ExAC. The bar graph on the left compares the frequency of variant positive individuals in the ExAC (23/60,706; 0.04%) to our LQTS cohort (6/39; 15.4%; p<0.0001).

Figure 2: Demographic and clinical characteristics of the CaM-positive patients. **(A)** Bar graph comparing average age of diagnosis for our CaM-negative cases (23 ± 3 years), and CaM-positive cases (0.67 ± 0.7 years; $p < 0.01$). **(B)** Bar graph comparing the percent CaM-positive patients < 5 years of age (6/10; 60%) to patients ≥ 5 years of age (0/29; 0%; $p < 0.0001$). **(C)** Bar graph comparing the QTc of CaM negative patients (514 ± 9 ms) to CaM-positive patients (679 ± 32 ms; $p < 0.0001$). **(D)** Pie charts comparing the number of patients who had experienced cardiac arrest in our CaM-negative (8/33; 24%) versus CaM-positive patients (6/6; 100%; $p < 0.001$). Data in **(A)** and **(B)** are shown as mean ± SEM.

Figure 3: Ca^{2+} titration curves for WT- and E141G-CaM and patch clamp analysis in TSA201 cells. **(A)** Data were used to derive dissociation constants (K_d, in μM) for the each domain. E141G-CaM led to an 11-fold reduction in Ca^{2+} affinity of CaM C-domain compared to WT-CaM, whereas N-domain Ca^{2+} binding was not statistically different. Values are averages of 3 experiments, and error was determined by analysis of the curve fits. **(B)** Representative tracings of whole cell $Ca_V1.2$ current from TSA201 cells expressing $Ca_V1.2$+EV, $Ca_V1.2$+WT-CaM and $Ca_V1.2$+E141G-CaM determined from a holding potential -90 mV to testing potential of +70 mV in 10 mV increments with 500 ms duration. **(C)** Current-voltage relationship for $Ca_V1.2$+EV, $Ca_V1.2$+WT-CaM, and $Ca_V1.2$+E141G-CaM. All values represent mean ± SEM. **(D)**

Inactivation-activation curves of $Ca_V1.2$+EV, $Ca_V1.2$+WT-CaM and $Ca_V1.2$+E141G-CaM (n=8-12). Steady-state inactivation was determined from a holding potential of -90 mV to pre-pulse of 20 mV in 10 mV increments with 10 s duration followed by a test pulse of 30 mV with 500 ms duration. I/Imax represents normalized calcium current and G/Gmax represents normalized conductance. Fast **(E)** and slow **(F)** decay time of $Ca_V1.2$+EV, $Ca_V1.2$+WT-CaM and $Ca_V1.2$+E141G-CaM. *P<0.05 vs. $Ca_V1.2$+WT-CaM.

Figure 4: E141G-CaM leads to increased $Ca_V1.2$ persistent current and alters current inactivation without affecting peak current density in murine ventricular myocytes. **(A)** Representative tracings of persistent $Ca_V1.2$ current from $Ca_V1.2$+EV, $Ca_V1.2$+WT-CaM and $Ca_V1.2$+E141G-CaM determined from a holding potential of -90 mV to +30 mV with 500ms duration in TSA201 cells. **(B)** Group data showing $Ca_V1.2$ late current normalized to peak (%) for $Ca_V1.2$+EV, $Ca_V1.2$+WT-CaM, and $Ca_V1.2$+E141G-CaM in TSA201 cells. *P<0.05 vs. $Ca_V1.2$+WT-CaM. **(C)** Representative examples of traces for each experimental group in murine ventricular myocytes. **(D)** Average current densities (pA/pF) obtained in cells dialyzed with WT- or E141G-CaM in murine ventricular myocytes. **(E)** Effect of E141G-CaM alone or mixed with 75% WT CaM on inactivation time constant of the $Ca_V1.2$ compared to WT-CaM in murine ventricular myocytes. Data are mean ± SD. (n=7 *P<0.05; †P<0.001 *vs.* WT-CaM. ‡P<0.01 *vs.* E141G-CaM alone).

Figure 5: E141G-CaM leads to increased $Na_V1.5$ late current. **(A)** Representative tracings of whole cell $Na_V1.5$ current from TSA201 cells expressing $Na_V1.5$+EV, $Na_V1.5$+WT-CaM, and $Na_V1.5$+E141G-CaM determined from a holding potential of -100 mV to testing potential of +90

mV in 10 mV increments with 24 ms duration. **(B)** Current-voltage relationship for $Na_V1.5$+EV, $Na_V1.5$+WT-CaM, and $Na_V1.5$+E141G-CaM. All values represent mean ± SEM. **(C)** Inactivation-activation curves of $Na_V1.5$+EV, $Na_V1.5$+WT-CaM and $Na_V1.5$+E141G-CaM (n=13-15). Steady-state inactivation obtained from a holding potential of -120 mV to pre-pulse of 0 mV in 10 mV increments with 976 ms duration followed by a test pulse of 0 mV with 24 ms duration. I/Imax represents normalized sodium current, G/Gmax represents normalized conductance. **(D)** Fast and slow decay time of $Na_V1.5$+EV, $Na_V1.5$+WT-CaM, and $Na_V1.5$+E141G-CaM. **(E)** Representative tracings of $Na_V1.5$ late current from $Na_V1.5$+EV, $Na_V1.5$+WT-CaM, $Na_V1.5$+E141G-CaM, and $Na_V1.5$+WT-CaM+E141G-CaM determined from a holding potential of -120 mV to -20 mV with 700ms duration. **(F)** Group data showing $Na_V1.5$ late current normalized to peak (%) for $Na_V1.5$+EV, $Na_V1.5$+WT-CaM, $Na_V1.5$+E141G-CaM, and $Na_V1.5$+WT-CaM+E141G-CaM. *P<0.05 vs. $Na_V1.5$+WT-CaM.

Figure 6: E141G-CaM has no effect on Ca^{2+} sparks and SR Ca^{2+} content. **(A)** Representative line-scan images of Ca^{2+} sparks in permeabilized mouse ventricular myocytes in CaM-free (vehicle), WT-CaM, and E141G-CaM in the presence of AIP2 (1μM). **(B)** Average Ca^{2+} spark frequency and **(C)** Ca^{2+} spark amplitude. Data are mean ± SD (n=20). **(D)** Line scan (top) and (bottom) line plot (red arrow) examples of SR Ca^{2+} content evaluated by 10 mM caffeine-evoked Ca^{2+} transient in CaM-free (vehicle), WT-CaM, and E141G-CaM in the presence of AIP2 (1μM). **(E)** Average SR Ca^{2+} content. Data are mean ± SD (n=4).

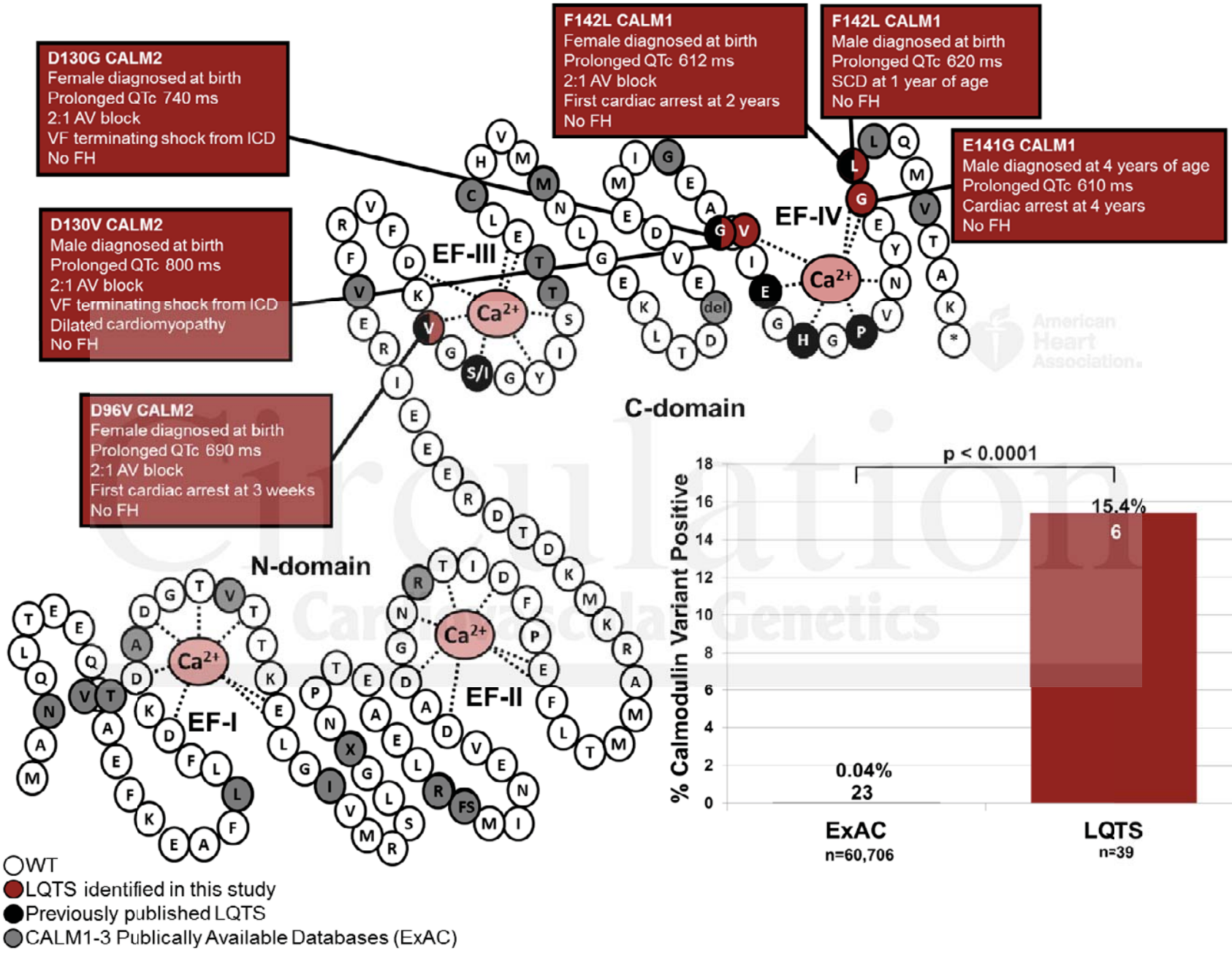
D130G CALM2
Female diagnosed at birth
Prolonged QTc 740 ms
2:1 AV block
VF terminating shock from ICD
No FH
D130V CALM2
Male diagnosed at birth
Prolonged QTc 800 ms
2:1 AV block
VF terminating shock from ICD
Dilated cardiomyopathy
No FH
D96V CALM2
Female diagnosed at birth
Prolonged QTc 690 ms
2:1 AV block
First cardiac arrest at 3 weeks
No FH
F142L CALM1
Female diagnosed at birth
Prolonged QTc 612 ms
2:1 AV block
First cardiac arrest at 2 years
No FH
F142L CALM1
Male diagnosed at birth
Prolonged QTc 620 ms
SCD at 1 year of age
No FH
E141G CALM1
Male diagnosed at 4 years of age
Prolonged QTc 610 ms
Cardiac arrest at 4 years
No FH
EF-I
EF-II
EF-III
EF-IV
N-domain
C-domain
Ca2+
p < 0.0001
% Calmodulin Variant Positive
0.04%
23
15.4%
6
ExAC
n=60,706
LQTS
n=39
WT
LQTS identified in this study
Previously published LQTS
CALM1-3 Publically Available Databases (ExAC)

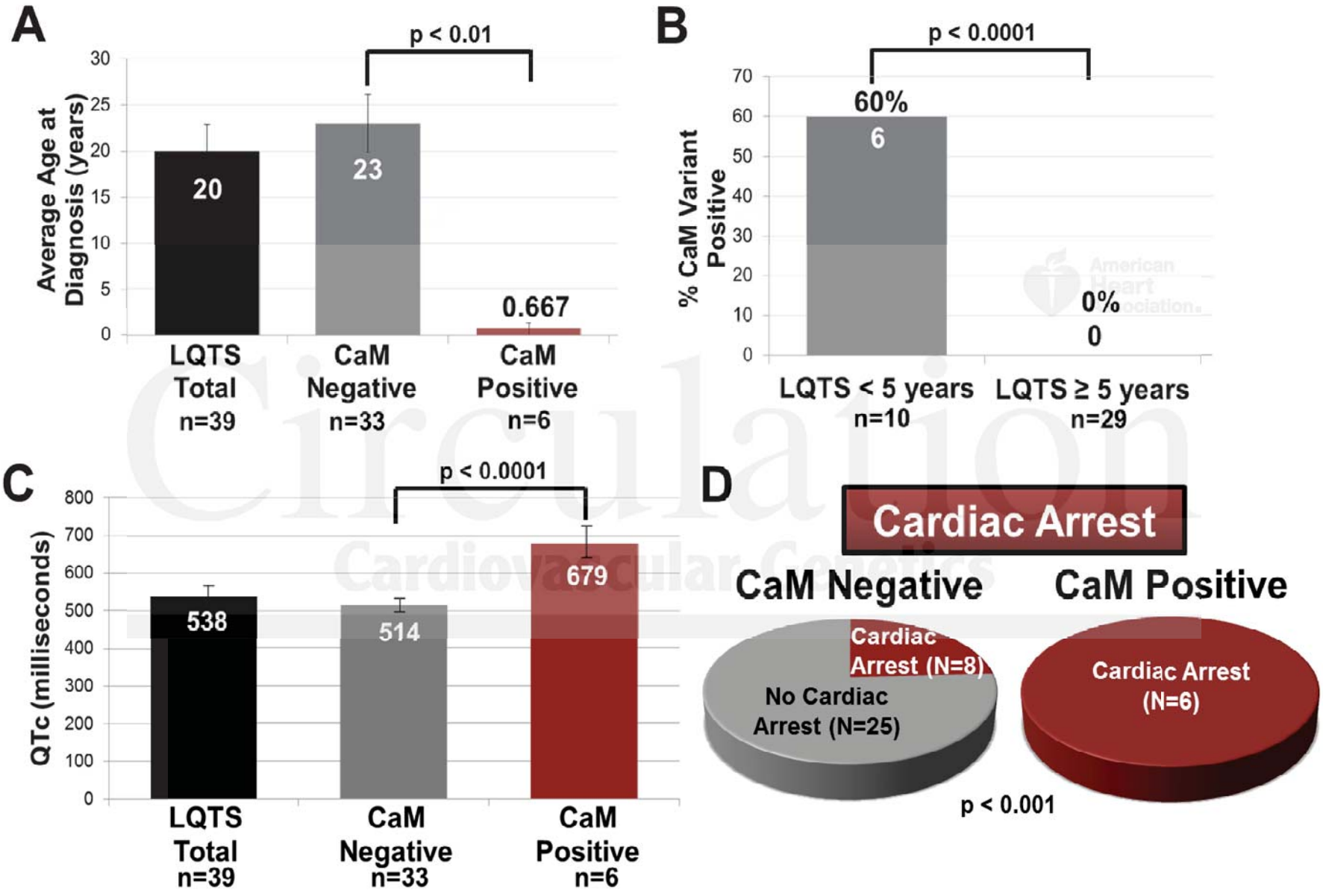
A
p < 0.01
Average Age at Diagnosis (years)
30
25
20
15
10
5
0
20
23
0.667
LQTS Total n=39
CaM Negative n=33
CaM Positive n=6
B
p < 0.0001
% CaM Variant Positive
70
60
50
40
30
20
10
0
60%
6
0%
0
LQTS < 5 years n=10
LQTS ≥ 5 years n=29
C
p < 0.0001
QTc (milliseconds)
800
700
600
500
400
300
200
100
0
538
514
679
LQTS Total n=39
CaM Negative n=33
CaM Positive n=6
D
Cardiac Arrest
CaM Negative
CaM Positive
Cardiac Arrest (N=8)
No Cardiac Arrest (N=25)
Cardiac Arrest (N=6)
p < 0.001

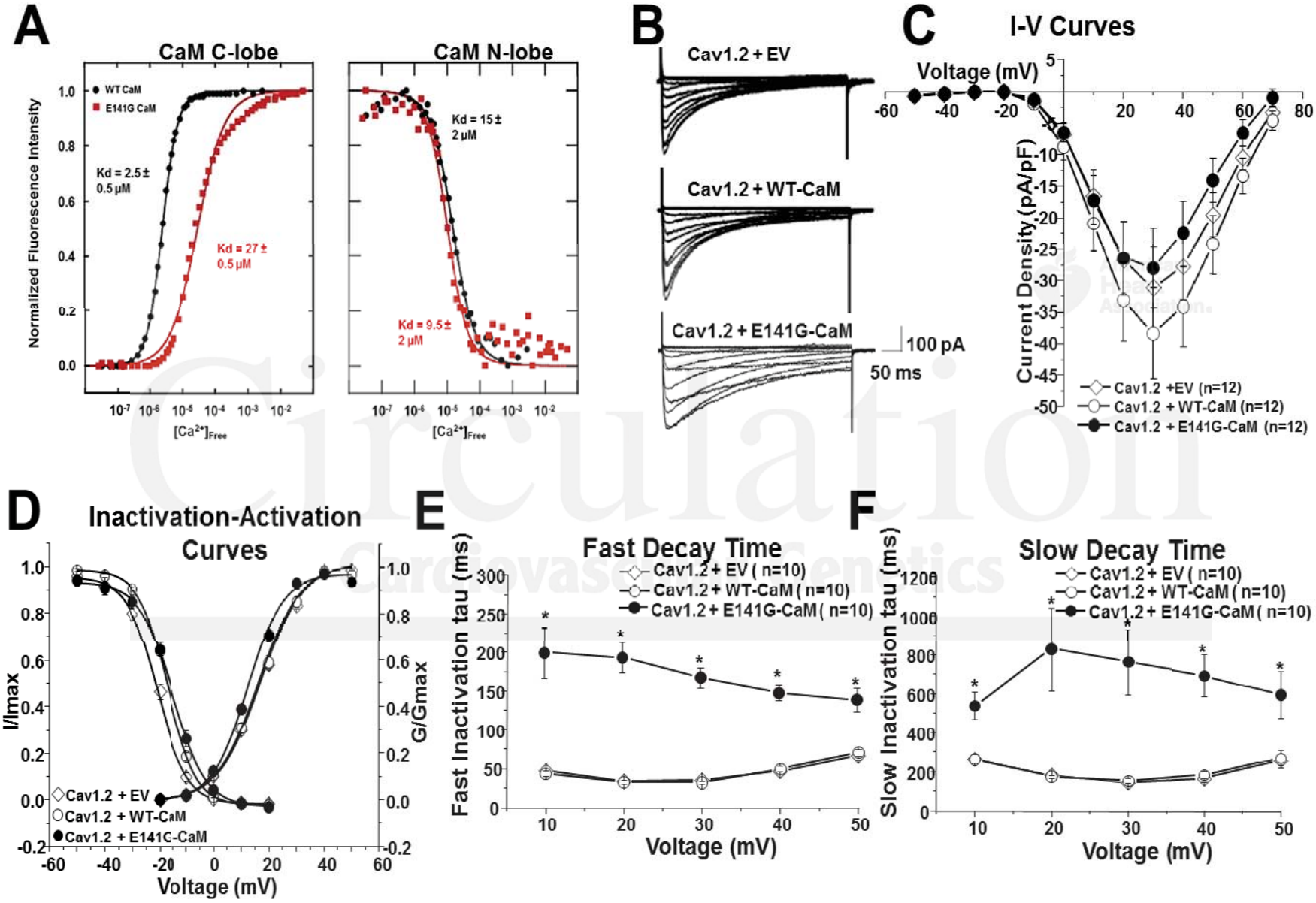
A
CaM C-lobe
CaM N-lobe
WT CaM
E141G CaM
Kd = 2.5 ± 0.5 µM
Kd = 27 ± 0.5 µM
Kd = 15 ± 2 µM
Kd = 9.5 ± 2 µM
Normalized Fluorescence Intensity
[Ca2+]Free
B
Cav1.2 + EV
Cav1.2 + WT-CaM
Cav1.2 + E141G-CaM
100 pA
50 ms
C
I-V Curves
Voltage (mV)
Current Density (pA/pF)
Cav1.2 +EV (n=12)
Cav1.2 + WT-CaM (n=12)
Cav1.2 + E141G-CaM (n=12)
D
Inactivation-Activation Curves
I/Imax
G/Gmax
Voltage (mV)
Cav1.2 + EV
Cav1.2 + WT-CaM
Cav1.2 + E141G-CaM
E
Fast Decay Time
Fast Inactivation tau (ms)
Cav1.2 + EV (n=10)
Cav1.2 + WT-CaM (n=10)
Cav1.2 + E141G-CaM (n=10)
Voltage (mV)
F
Slow Decay Time
Slow Inactivation tau (ms)
Cav1.2 + EV (n=10)
Cav1.2 + WT-CaM (n=10)
Cav1.2 + E141G-CaM (n=10)
Voltage (mV)

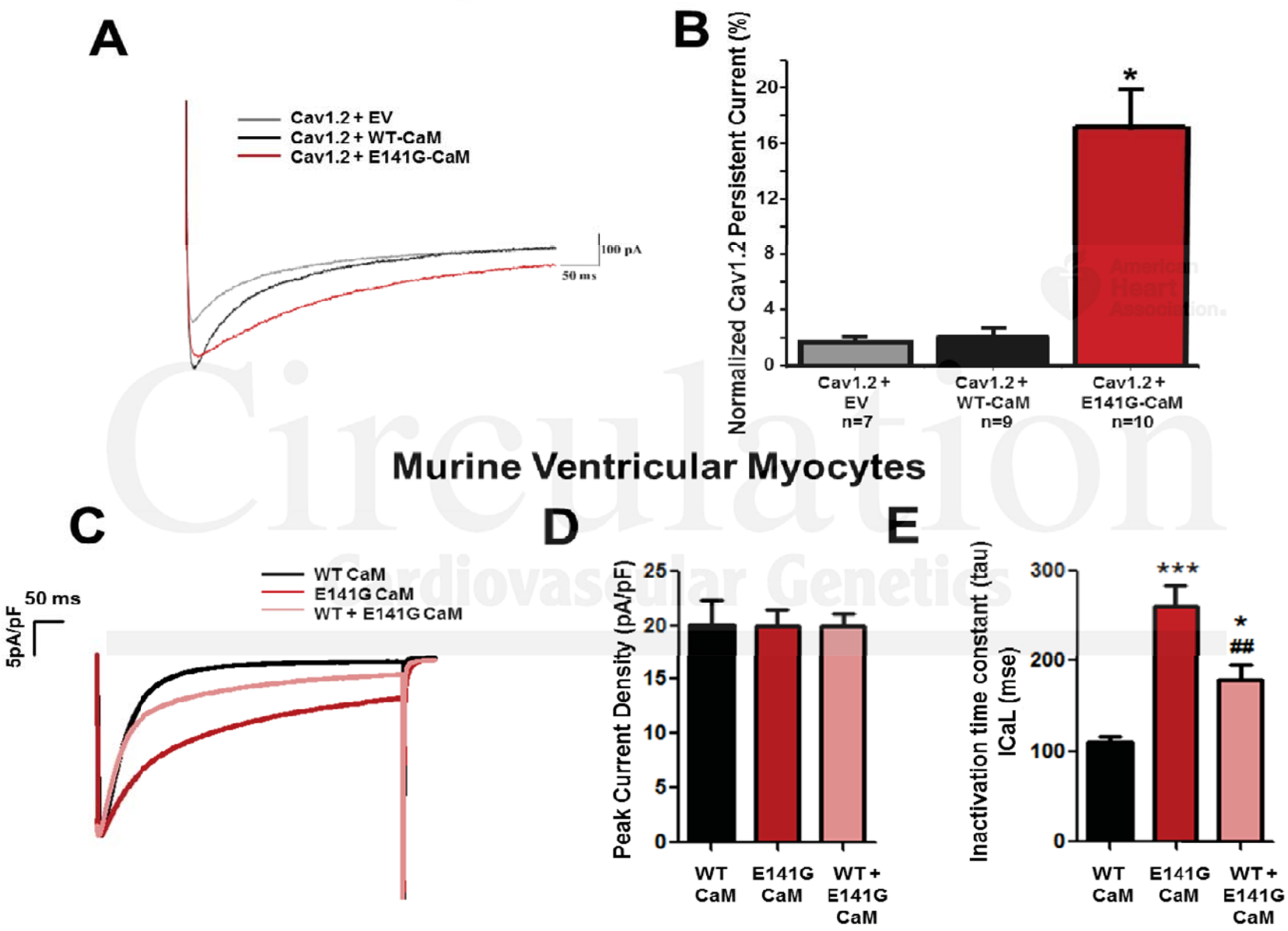
Heterologous Expression in TSA201 Cells
A
Cav1.2 + EV
Cav1.2 + WT-CaM
Cav1.2 + E141G-CaM
100 pA
50 ms
B
Normalized Cav1.2 Persistent Current (%)
20
16
12
8
4
0
*
Cav1.2 + EV n=7
Cav1.2 + WT-CaM n=9
Cav1.2 + E141G-CaM n=10
Murine Ventricular Myocytes
C
WT CaM
E141G CaM
WT + E141G CaM
50 ms
5pA/pF
D
Peak Current Density (pA/pF)
25
20
15
10
5
0
WT CaM
E141G CaM
WT + E141G CaM
E
Inactivation time constant (tau) ICaL (mse)
300
200
100
0
***
*
##
WT CaM
E141G CaM
WT + E141G CaM

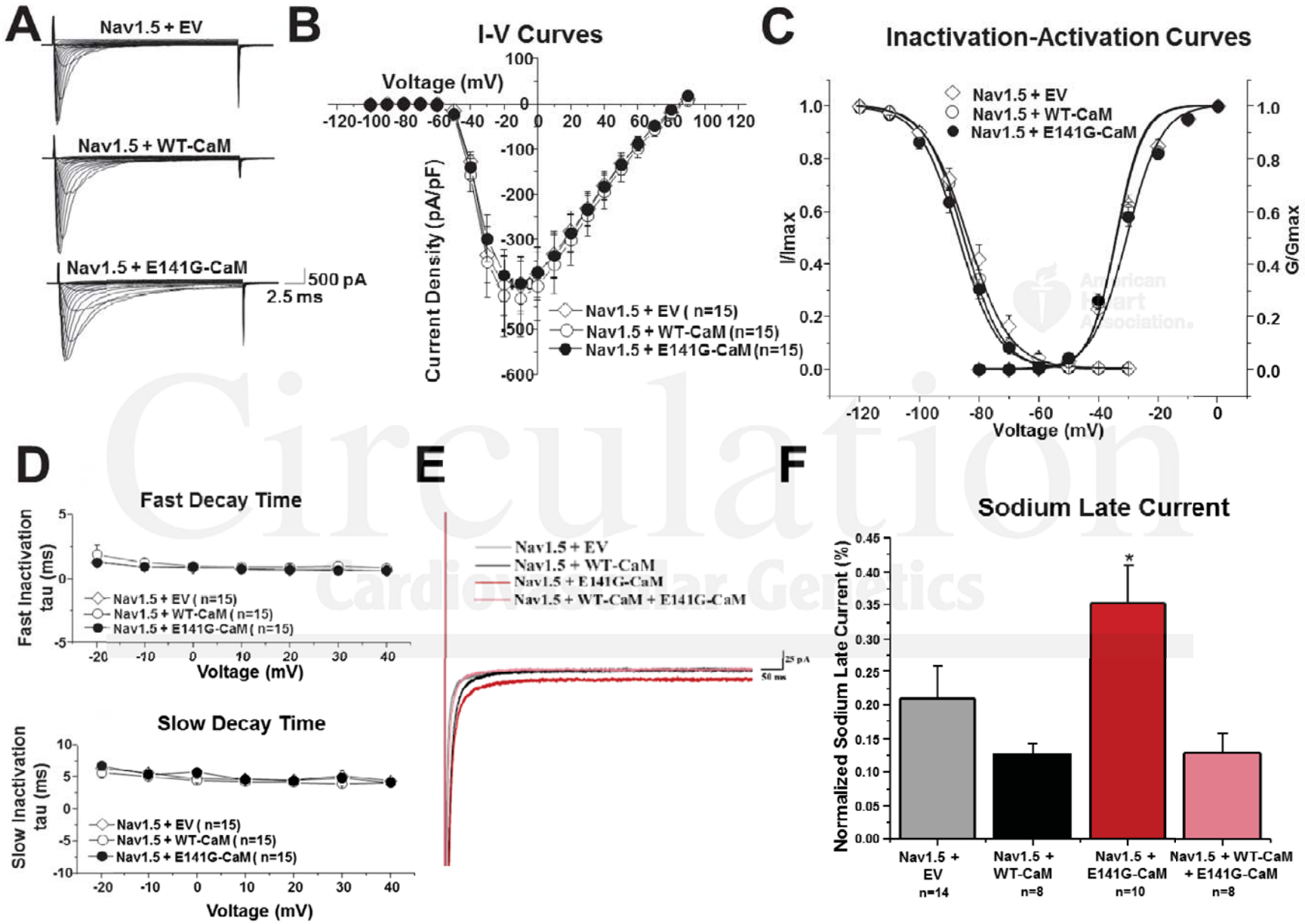
A
Nav1.5 + EV
Nav1.5 + WT-CaM
Nav1.5 + E141G-CaM
500 pA
2.5 ms
B
I-V Curves
Voltage (mV)
Current Density (pA/pF)
Nav1.5 + EV (n=15)
Nav1.5 + WT-CaM (n=15)
Nav1.5 + E141G-CaM (n=15)
C
Inactivation-Activation Curves
Nav1.5 + EV
Nav1.5 + WT-CaM
Nav1.5 + E141G-CaM
I/Imax
G/Gmax
Voltage (mV)
D
Fast Decay Time
Fast Inactivation tau (ms)
Nav1.5 + EV (n=15)
Nav1.5 + WT-CaM (n=15)
Nav1.5 + E141G-CaM (n=15)
Voltage (mV)
Slow Decay Time
Slow Inactivation tau (ms)
Nav1.5 + EV (n=15)
Nav1.5 + WT-CaM (n=15)
Nav1.5 + E141G-CaM (n=15)
Voltage (mV)
E
Nav1.5 + EV
Nav1.5 + WT-CaM
Nav1.5 + E141G-CaM
Nav1.5 + WT-CaM + E141G-CaM
25 pA
50 ms
F
Sodium Late Current
Normalized Sodium Late Current (%)
*
Nav1.5 + EV n=14
Nav1.5 + WT-CaM n=8
Nav1.5 + E141G-CaM n=10
Nav1.5 + WT-CaM + E141G-CaM n=8

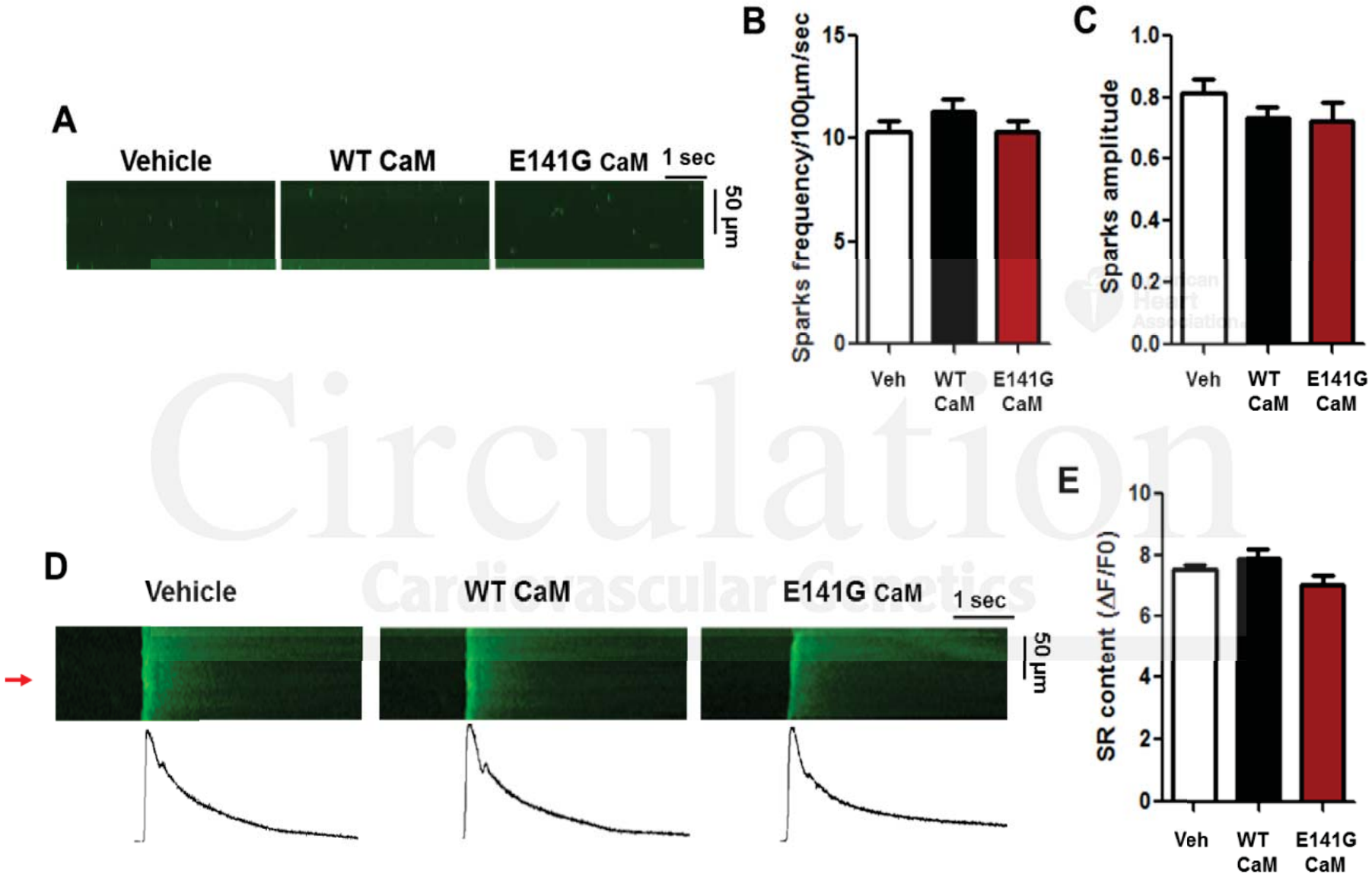
A
Vehicle
WT CaM
E141G CaM
1 sec
50 μm
B
Sparks frequency/100μm/sec
15
10
5
0
Veh
WT CaM
E141G CaM
C
Sparks amplitude
1.0
0.8
0.6
0.4
0.2
0.0
Veh
WT CaM
E141G CaM
D
Vehicle
WT CaM
E141G CaM
1 sec
50 μm
E
SR content (ΔF/F0)
10
8
6
4
2
0
Veh
WT CaM
E141G CaM